



Universiteit
Leiden
The Netherlands

Percutaneous endovascular delivery of calcium chloride to the intact porcine carotid artery: a novel animal model of arterial calcification

Abrao, S.R.; Campos, C.M.; Cavalcante, R.; Eggermont, J.; Lemos, P.; Lederman, A.; ... ; Brito, F.S.D.

Citation

Abrao, S. R., Campos, C. M., Cavalcante, R., Eggermont, J., Lemos, P., Lederman, A., ... Brito, F. S. D. (2020). Percutaneous endovascular delivery of calcium chloride to the intact porcine carotid artery: a novel animal model of arterial calcification. *Catheterization & Cardiovascular Interventions*, 96(4), E484-E492. doi:10.1002/ccd.29070

Version: Publisher's Version
License: [Creative Commons CC BY 4.0 license](https://creativecommons.org/licenses/by/4.0/)
Downloaded from: <https://hdl.handle.net/1887/3184246>

Note: To cite this publication please use the final published version (if applicable).

Percutaneous endovascular delivery of calcium chloride to the intact porcine carotid artery: A novel animal model of arterial calcification

Sérgio R. Abrão MD¹ | Carlos M. Campos MD, PhD^{1,2}  |
 Rafael Cavalcante MD, PhD³ | Jeroen Eggermont PhD⁴ | Pedro Lemos MD, PhD^{1,2} |
 Alex Lederman MD, PhD^{1,5} | Erasmo S. da Silva MD, PhD⁵ |
 Ricardo Aun MD, PhD^{1,5} | Sergio Q. Belczak MD, PhD^{1,3} |
 Alexandre Abizaid MD, PhD² | Fabio Sandoli de Brito Jr MD, PhD^{2,3} 

¹Hospital Israelita Albert Einstein, Sao Paulo, Brazil

²Heart Institute (InCor), University of São Paulo Medical School, Sao Paulo, Brazil

³Hospital Sao Camilo, Sao Paulo, Brazil

⁴Leiden University Medical Center, Leiden, The Netherlands

⁵Department of Vascular Surgery, University of São Paulo Medical School, Sao Paulo, Brazil

Correspondence

Fabio Sandoli de Brito Jr, MD, PhD,
 Department Interventional Cardiology, Heart
 Institute, University of São Paulo Medical
 School, Av. Dr Enéas Carvalho de Aguiar
 44, São Paulo, Brazil.
 Email: fabio.cardiol@gmail.com

Funding information

Fundação de Amparo à Pesquisa do Estado de São Paulo

Abstract

Objective: The present study evaluated the effect of endovascular administration of calcium chloride to the carotid artery of swines, to create a model of arterial calcification.

Methods: Fifteen Large White pigs were used for the study. Via endovascular treatment, carotid arteries were exposed during 9 min to either calcium chloride (experimental artery) or saline (control artery) with the use of the TAPAS catheter. Intravascular ultrasound (IVUS) imaging was obtained at baseline, postprocedure and at 30 days. Optical coherence tomography (OCT) imaging was obtained in vitro after carotids were harvested. Longitudinally cut parallel arterial segments were placed in a system of delicate clamps and underwent uniaxial strain test. All arteries underwent histopathological examination.

Results: Calcium chloride treated segments showed extensive circumferential parietal calcification evident on both IVUS and OCT. Reduction in minimal lumen area on IVUS was evident in experimental arteries both at 24 hr and 30 days postprocedure. Histopathologic assessment (Von Kossa stain) confirmed medial calcification with mild intimal thickening. Biomechanical testing showed treated segments to have smaller breaking strength and less elastic deformation than controls.

Conclusion: We developed a nonexpensive, reproducible model of early carotid medial calcification in pigs. Our model has the potential to help the development of research to unravel mechanisms underlying arterial calcification, the use of current or new devices to treat calcified lesions as well as to serve as an option for training interventionalists on the use of such devices.

KEYWORDS

biomechanics, experimental, histopathology, intravascular imaging

1 | INTRODUCTION

The use of animal models in interventional vascular medicine has contributed to increase our knowledge and to develop new devices and less invasive therapeutic options for patients with cardiovascular diseases. Several models have been developed to study atherosclerotic diseases, restenosis and vascular healing after balloon angioplasty and stenting, vascular aneurysms and heart failure, to name only a few.^{1,2}

Arterial calcification increases the likelihood of percutaneous intervention failure and complications and is associated with increased cardiovascular morbidity and mortality.³⁻⁷ Additionally, calcification may interfere with drug distribution and absorption in the vessel wall when using drug eluting stents and balloons.⁸ Therefore, an *in vivo* animal model of local arterial calcification would be useful for the evaluation of the efficacy and safety of new drugs and devices as well as for training purposes of physicians to perform interventional procedures with dedicated devices for calcified lesion preparation.

It has been previously shown that periadventitial treatment of the rat abdominal aorta with low concentrations of calcium chloride induced calcification of vascular elastic fibers.⁹ The present study evaluated the effect of local administration of calcium chloride to the carotid wall of swines, with the objective of creating a novel animal model of arterial calcification.

2 | METHODS

The study was conducted at the Animals experiment laboratory of the Hospital Israelita Albert Einstein in Sao Paulo, Brazil. Biomechanics testing was performed at the Department of Surgery of the University of Sao Paulo Medical School. The Hospital Israelita Albert Einstein Imaging Core Laboratory analyzed all intravascular images. The ethics committee on the use of laboratory animals approved the research protocol.

2.1 | Study population

The study was conducted in two separate phases and included in total 20 male Large White pigs (average weight = 57.8 ± 9.5 kg). In the first phase, five animals (pilot group) were used for protocol and technique adjustments. The second phase included 15 pigs divided into three groups as follows: Study Group 1 (10 pigs)—animals underwent intravascular ultrasound (IVUS) assessment pre and post procedure and at 30-day follow-up. At this point the pigs were euthanized for harvesting the carotid arteries for anatomopathologic and biomechanic evaluations; Study Group 2 (three pigs)—after euthanasia at 30 days, carotid arteries were harvested for *in vitro* assessment with OCT and histopathologic examination; Study Group 3 (two pigs)—animals were euthanized after 24 hr postprocedure for OCT and histopathologic evaluation as in Group 2.

2.2 | Study animal preparation

Healthy Large White pigs were sedated with intramuscular administration of ketamine 20 mg/kg plus midazolam 0.05 mg/kg. After asepsis, pigs were weighted and taken to the operating room. Anesthesia was obtained and maintained with isoflurane $\leq 1.5\%$ with the pigs under mechanical ventilation. Antibiotic prophylaxis was achieved with 2 g of ceftriaxone. All interventions were conducted under sterile conditions.

2.3 | Interventional procedure

Ultrasound guided puncture of the right common femoral artery was used for arterial access with the insertion of a 100 cm 10F sheath. A bolus of 10 000 UI of unfractionated heparin was given. Subsequently, selective angiography of both common carotid arteries was performed and IVUS imaging was obtained with the Opticross 40 MHz catheter (Boston Scientific, Marlborough, Massachusetts). Images were acquired with an automatic pullback at a speed of 0.5 mm/s. The first common carotid artery to be selectively engaged (right or left) received calcium chloride infusion and the contra-lateral one received saline infusion (control).

The TAPAS catheter (Termopeutix Inc., San Diego, California) with double balloon was inserted and positioned at the common carotid artery and its balloons filled with contrast. Blood was aspirated from the 40 mm long lumen between the two balloons, which were filled with calcium chloride (intervention artery) or saline (control artery).^{10,11} After 9 min, the fluids were aspirated and blood flow was restored by deflating the balloons. All pigs were treated daily with dual antiplatelet therapy with aspirin 100 mg and clopidogrel 75 mg.

2.4 | Intravascular imaging analysis

Intravascular ultrasound images were assessed offline by an independent corelab. QIVUS software (Medis, Leiden, The Netherlands) was used for all analysis. Optical coherence tomography (OCT) images were obtained *in vitro* from the harvested arteries after pigs were euthanized. Images were assessed qualitatively for the presence of arterial calcification. The Hospital Israelita Albert Einstein Imaging Core Laboratory analyzed all intravascular images. IVUS images were assessed offline by the QCU-CMS-Research v4.69 (Leiden, The Netherlands). Images were assessed qualitatively for the presence of arterial calcification. Additionally, automatic echogenicity was assessed for tissue classification. The methodology of echogenicity has been described elsewhere.¹² Echogenicity aims to classify the vessel wall components located between the luminal boundary and the external elastic membrane (EEM) into two or more categories based on their gray-level intensity in B-mode IVUS images rather than based on radiofrequency ultrasound signal analysis. Here, we quantify four tissue types: hypoechogenic,

hyperechogenic, calcified, and unknown. Hypo- and hyperechogenic areas are classified based on their gray-level intensities relative to the median gray-level intensity of the adventitia (darker or brighter than adventitia, respectively). The presence of hyperechogenic areas surrounded by acoustic shadows is classified as calcium. The tissue in the acoustic shadow was classified as unknown. Efforts were made to offset the impact of variable baseline artery size and vessel growth over time. Thus, vessel dimensions at follow-up were normalized using nonintervened carotids references as an attempt to normalize the changes in vessel morphometry over time as previously described.¹³

2.5 | Histopathology

All carotid arteries were harvested and underwent careful surgical dissection of all pericarotid tissue. Subsequently, arteries were sectioned longitudinally producing two arterial segments of each harvested carotid for histopathological analysis and biomechanical testing. For histopathologic assessment the following stains were used: Hematoxylin-eosin (HE), Verhoeff, Picrosirius, Masson's Trichrome, and Von Kossa.

2.6 | Biomechanical testing

Longitudinally cut parallel arterial segments were placed in a system of delicate clamps and underwent uniaxial strain test controlled by the SERIES IX and INSPEC softwares as previously described.¹⁴⁻¹⁷

2.7 | Statistical analysis

Continuous variables are presented as mean \pm SD and compared with paired *t* test. Categorical variables are presented as counts (percentages) and compared with the Fisher test. Two-sided *p* values $<.05$ are

considered statistically significant. SPSS software V.21 (IBM) was used for all analyses.

3 | RESULTS

3.1 | Study population

At Phase 1 (pilot group), one pig had carotid occlusion following exposure to Calcium chloride and two other died, one of complications of surgery and the other of respiratory infection. At Phase 2, three pigs of study Group 1 were excluded due to early postoperative death (two cases) and failure of the Tapas catheter during calcium chloride infusion (one case). Therefore, the analysis of study Group 1 comprised seven pigs. In study Groups 2 and 3, all procedures were uneventful and euthanasia was performed at the planned time.

3.2 | Intravascular imaging

At baseline, no difference in IVUS parameters between the calcium chloride and saline groups were observed (Table 1). Immediately after procedure the experimental arteries demonstrated a significant reduction in both minimal lumen area (8.2 ± 6.0 vs. 21.1 ± 9.3 ; $p = .01$; treated vs. control, respectively) and mean lumen area (14.1 ± 9.4 vs. 24.6 ± 8.1 ; $p = .04$). At 1-month follow-up, treated segments showed extensive parietal calcification, characterized by a hyperechogenic image with acoustic shadowing (Figure 1). The average length of arterial segment with arc of calcium $\geq 300^\circ$ was 25.3 ± 12.3 mm, corresponding to $69 \pm 31\%$ of the segment exposed to CaCl_2 . Treated segments had a lower minimal lumen area (MLA) than controls both at postprocedure and at 30 days (Table 1). Due to the circumferential pattern of the calcification, external elastic membranes could not be identified, and remodeling patterns could not be determined. No morphologic modification was detected by gray scale IVUS in the control group (Figure 1 and Table 1).

	Calcium chloride (n = 7)	Saline control (n = 7)	<i>p</i> value
Baseline			
Mean lumen area, mm ²	24.0 \pm 7.0	25.5 \pm 7.0	.69
Minimal lumen area, mm ²	24.0 \pm 6.0	21.9 \pm 7.5	.92
Plaque burden, %	0.0 \pm 4.2	0.1 \pm 3.6	.95
Postprocedure			
Mean lumen area, mm ²	14.1 \pm 9.4	24.6 \pm 8.1	.04
Minimal lumen area, mm ²	8.2 \pm 6.0	21.1 \pm 9.3	.01
Plaque burden, %		19.5 \pm 22.9	
30-day follow-up			
Mean lumen area, mm ²	16.5 \pm 10.2	25.9 \pm 6.7	.06
Minimal lumen area, mm ²	12.6 \pm 8.0	23.5 \pm 6.4	.01
Plaque burden, %		7.2 \pm 5.6	

TABLE 1 Intravascular ultrasound findings

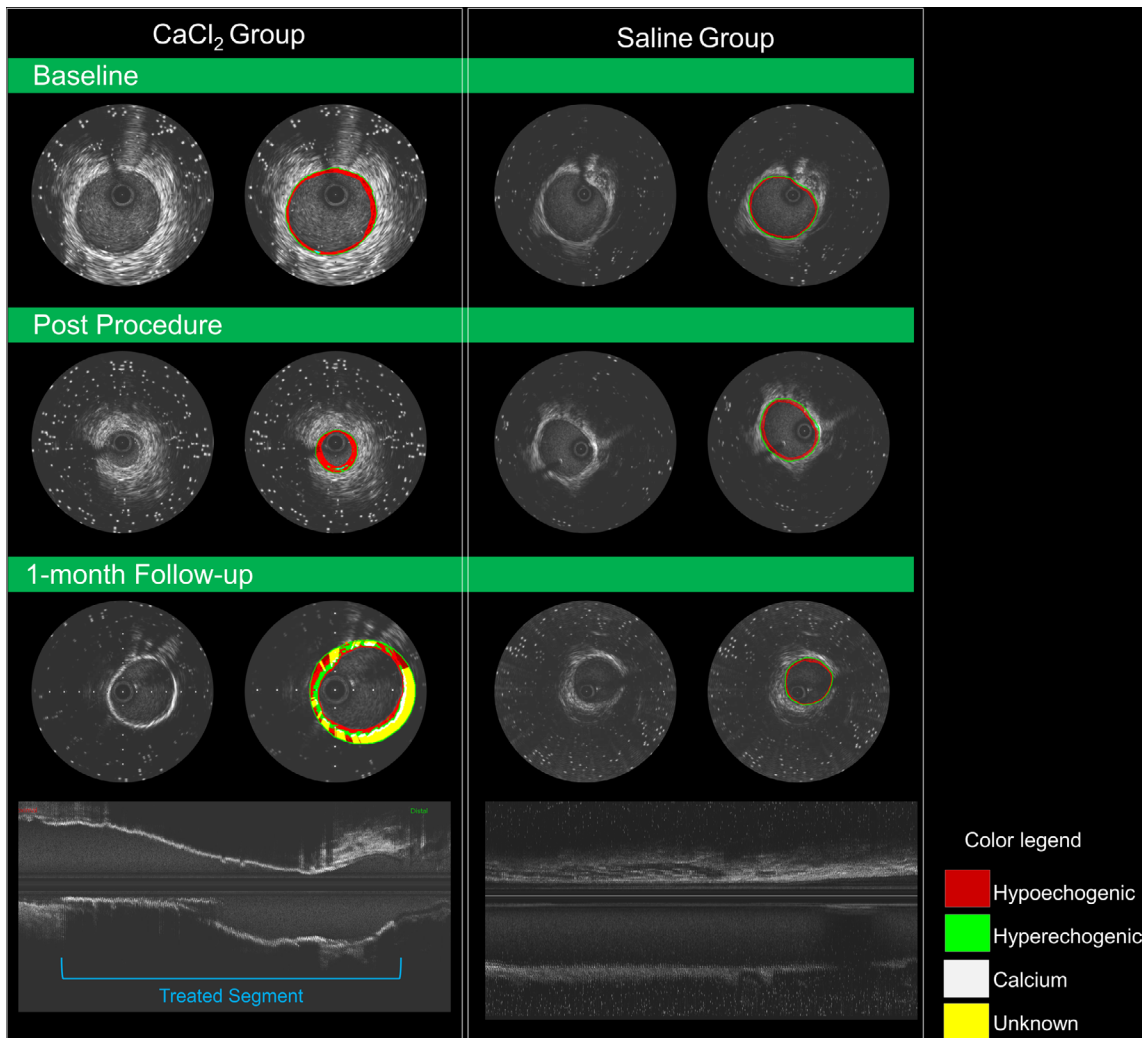


FIGURE 1 Intravascular ultrasound (IVUS) gray scale and echogenicity imaging at baseline, postprocedure and at 30 days. At baseline (top panel) the carotid of CaCl₂ (left) and Control (right) groups were similar, with a thin layer of hypoechoogenic tissue. The arteries treated with CaCl₂ had luminal reduction and infiltration of hyperechoogenic tissue post procedure. At 30-day follow-up, the experimental model demonstrated luminal reduction with extensive calcification in the treated region. In IVUS the gray-scale long-view image (bottom panel) the presence of acoustic shadow restricted to the region of interest is evident. Conversely, the control group had normal three-layered vessel pattern of the carotid artery

TABLE 2 Echogenicity findings

	Calcium chloride (n = 7)	Saline control (n = 7)	p value
Baseline			
Hyperechoogenic volume, mm ³	4.1 ± 1.1	4.1 ± 1.0	.9
Hypoechoogenic volume, mm ³	94.7 ± 22.6	94.3 ± 22.3	.8
Calcium volume, mm ³	0 ± 0	0 ± 0	1.0
Postprocedure			
Hyperechoogenic volume, mm ³	17.4 ± 6.4	4.6 ± 0.9	.03
Hypoechoogenic volume, mm ³	95.0 ± 20.7	94.8 ± 22.7	.8
Calcium volume, mm ³	1.2 ± 0.8	0.0 ± 0.1	.26
30-day follow-up			
Hyperechoogenic volume, mm ³	76.1 ± 9.8	2.6 ± 0.2	<.01
Hypoechoogenic volume, mm ³	118.9 ± 30.6	90.6 ± 17.6	<.01
Calcium volume, mm ³	16.6 ± 6.5	0.0 ± 0.1	<.01

Accordingly, IVUS echogenicity parameters of the two groups were similar at baseline (Table 2). After the procedure, there was a significant increase in the hyperechogenic volume in the experimental group (17.4 ± 6.4 vs. 4.6 ± 0.9 ; $p = .03$). At 1-month follow-up the calcium chloride group had significantly higher calcium volume (16.6

± 6.5 vs. 0.0 ± 0.1 ; $p < .01$) and hyperechogenic volume (118.9 ± 30.6 vs. 90.6 ± 17.6 ; $p < .01$).

On OCT, an image with well-defined borders denoting parietal calcification of the medial layer was evident in the treated segments at 30 days, but not 24 h after the procedure (Figure 2). Saline-injected

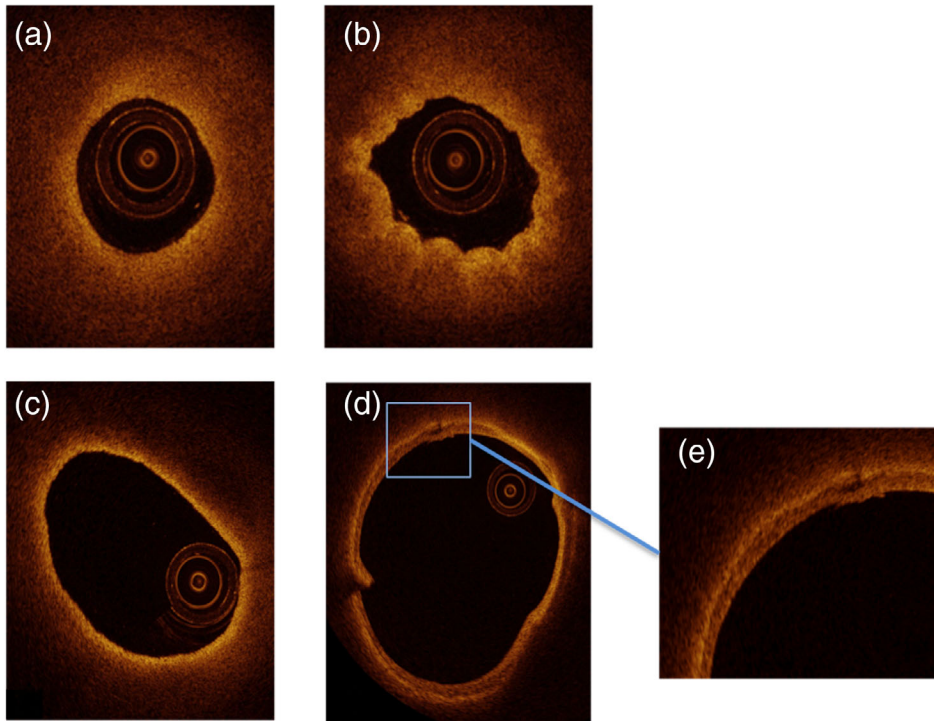


FIGURE 2 OCT imaging at 24 hr (upper panels) showing (a) a normal control artery and (b) a calcium chloride treated carotid. (c) Bottom panels show at 30 days a control and (d,e) a treated artery. On OCT, calcification of the tunica media is evident only at 30 days postprocedure and not after 24 hr

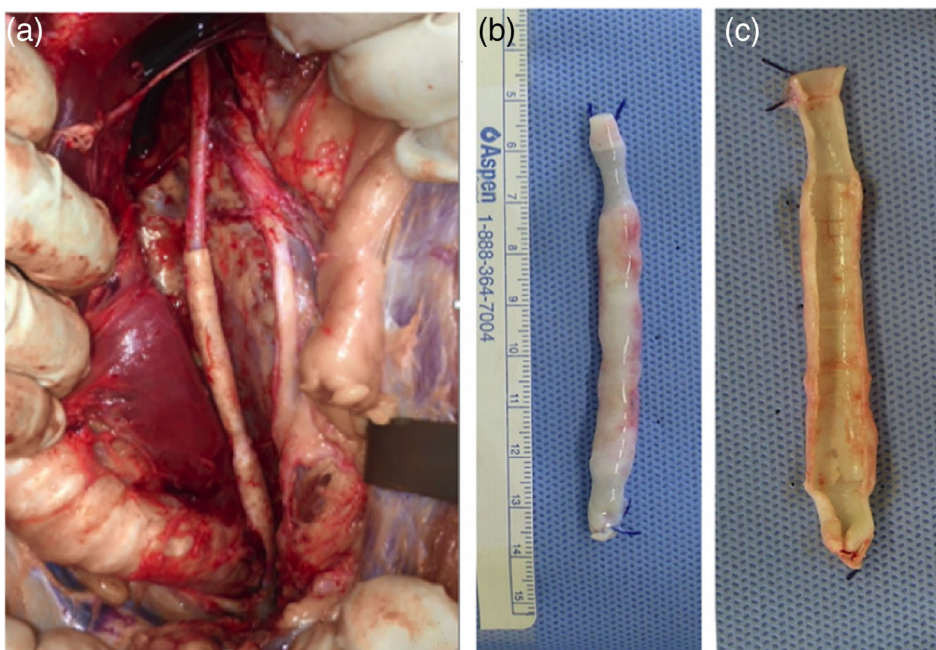


FIGURE 3 (a) In situ carotid artery exposed to calcium chloride showing a white pearly color. (b,c) After harvesting and longitudinal sectioning, intense calcification with cracks is observed

controls showed normal looking vessel on OCT assessment at both time points (Figure 2).

3.3 | Macroscopic evaluation

In situ macroscopic assessment of common carotid arteries revealed in all cases apparent increase in vessel diameter at the calcium chloride treated portions (as opposed to adjacent nontreated segments) when compared to control arteries that did not show this pattern. This can be explained by a caliber reduction in normal segments of the arteries after depressurization of the vessel

following euthanasia of the animals, which might have occurred to a lesser extent in calcified rigid segments exposed to calcium chloride. At visual and manual inspection, we observed a white pearly color and rigid, hardened texture of the CaCl_2 treated segments (Figure 3a). Longitudinal section of these segments revealed intense parietal calcification (Figure 3b,c).

3.4 | Histopathology

At 24 hr postprocedure (study Group 3), treated segments presented with a circumferential deposition of calcium at the most superficial

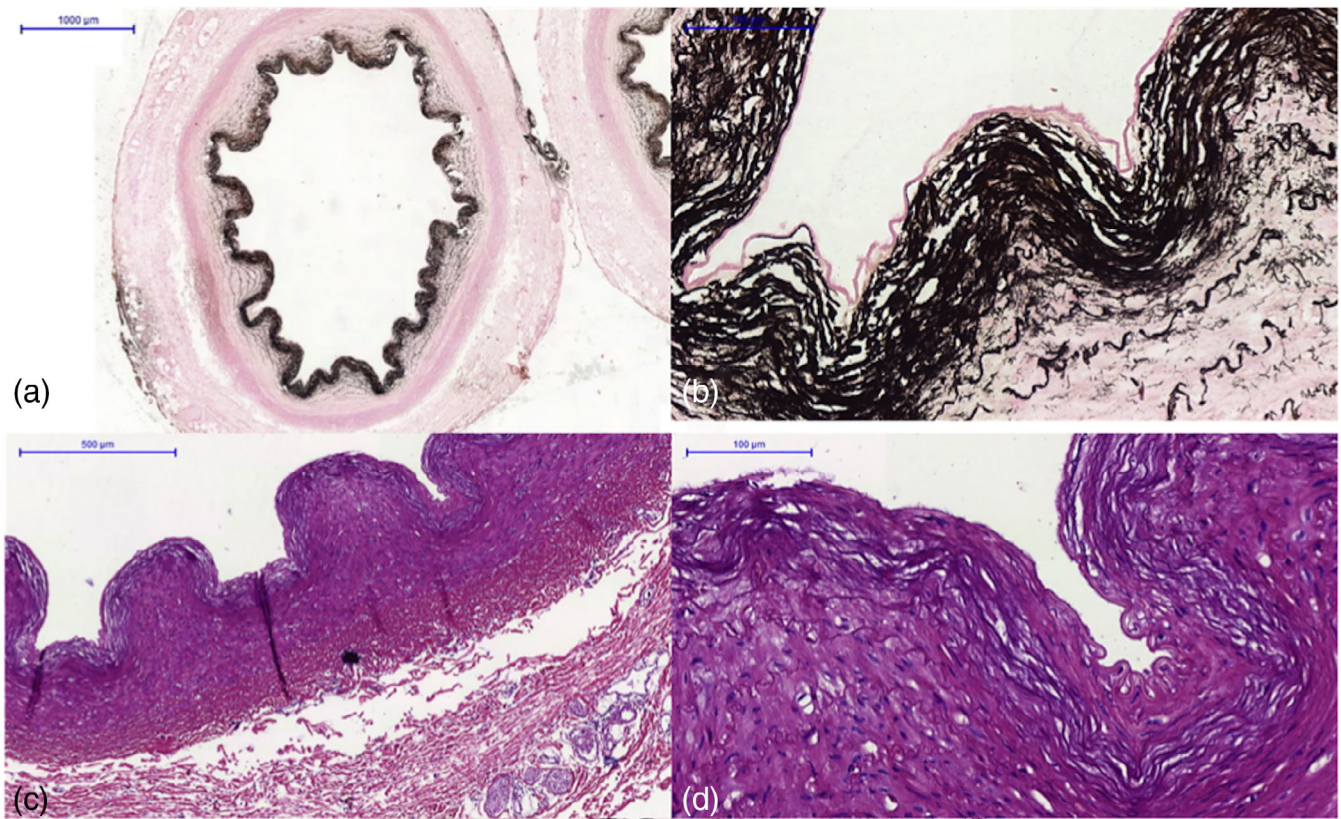


FIGURE 4 Histopathology of calcium exposed artery 24 hr postprocedure. (a,b) Calcification of elastic fibers (red arrows) is confirmed on the Von Kossa stain. (c,d) HE stain revealed necrosis of the inner portion of the tunica media (red arrows)

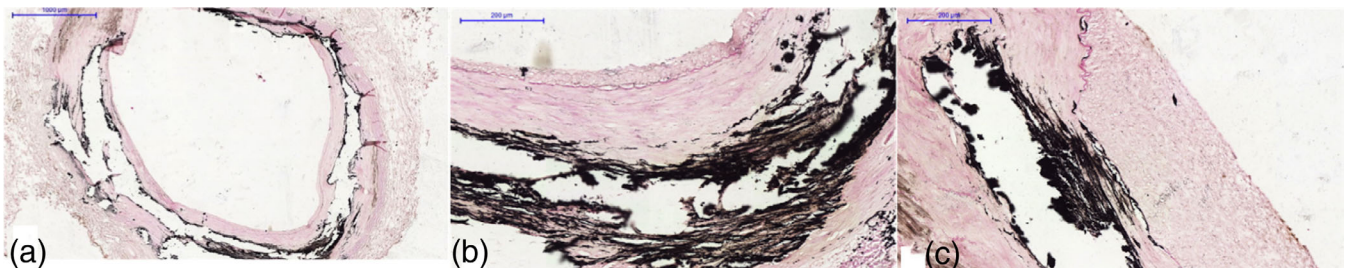


FIGURE 5 At 30 days, an intense, more organized circumferential calcification is noted. Mild intimal thickening is also observed (Von Kossa stain)

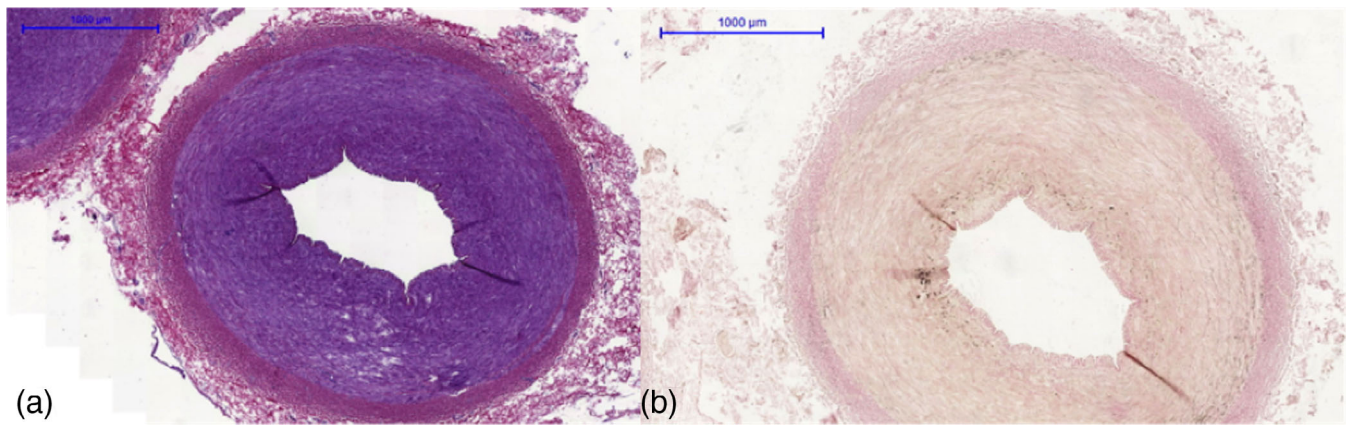


FIGURE 6 Histologically normal looking control artery on (a) HE and (b) Von Kossa stains

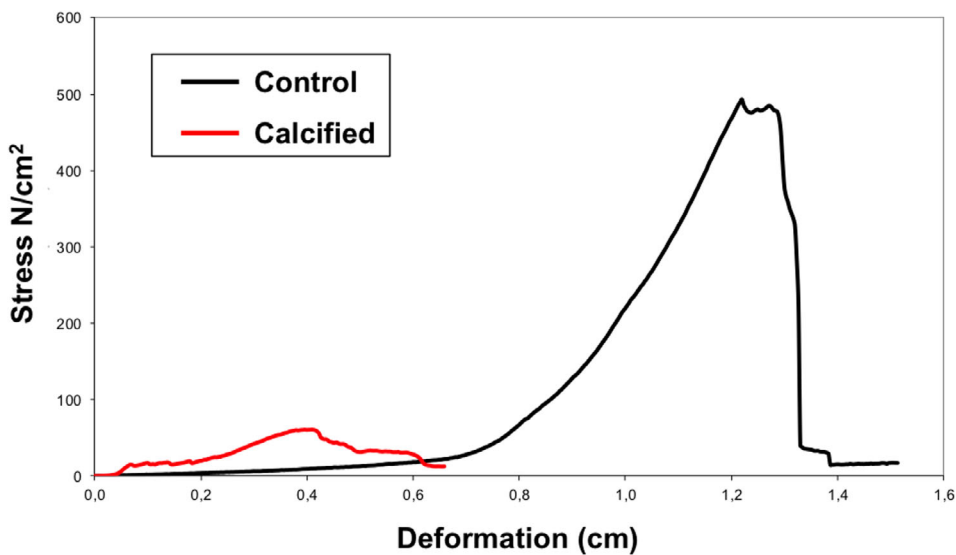


FIGURE 7 The graph depicts an example of the smaller breaking strength and elastic deformation of a calcium chloride treated artery in comparison with a control in the same animal

portion of the media layer below the internal elastic membrane. Von Kossa stain was positive (Figure 4a,b). Hematoxylin and eosin stain revealed necrosis of this inner half of media (Figure 4c,d). At 30 days (Study Groups 1 and 2), an organization of the initial process was apparent with circumferential calcification of the medial layer (Figure 5a) and mild intimal thickening (intimal hyperplasia) with proliferative tissue (star cells embedded in mucoid matrix) (Figure 5b,c). Saline injected arteries (controls) remained histologically normal (Figure 6a,b).

3.5 | Biomechanics

At biomechanical assessment, treated segments showed smaller breaking strength than controls (103.0 ± 63.1 vs. 373.9 ± 142.6 N/cm², respectively; $p = .004$) as well as less elastic deformation (0.4 ± 0.1 vs. 1.2 ± 0.1 cm, respectively; $p < .001$) (Figure 7).

4 | DISCUSSION

Calcification can affect arteries through different mechanisms. In coronary atherosclerosis, intimal calcification replacing lipid and necrotic tissue is recognized as an evolutionary disease process. In patients under secondary prevention with statins, for instance, this process is thought to reflect a stabilizing effect of lipid-lowering therapy.¹⁸⁻²⁰ In peripheral arteries, on the other hand, medial calcification can affect patients with diabetes and end-stage renal disease (ESRD) through a process that involves cell death at the tunica media.^{3,21}

Our study provides a model of carotid calcification in pigs that very much resemble the medial calcification naturally occurring in aging humans and more pronounced in those with diabetes and ESRD; the Monckeberg Sclerosis.²¹ The natural process is thought to occur following cell death through apoptosis, with elastin—present at the tunica media—serving as a nidus for the development of medial calcification.²¹ Histopathology of our model demonstrates, similarly, the occurrence of cell necrosis on the inner half of the tunica media

(HE stain) and circumferential medial calcification confirmed on the Von Kossa stain.

Additionally, luminal reduction was observed on IVUS in the segments exposed to calcium chloride. Although the external elastic membrane was not assessable due to the acoustic shadowing of the medial calcification, we can speculate that the mechanism of luminal reduction is, in the acute phase (24 hr) related to vessel spasm, and at 30 days due to negative remodeling associated with the healing process and calcification,²² since only minimal intimal hyperplasia was present.

Interestingly, the natural occurring process of vascular calcification in humans is thought to appear over long periods of time, being often associated with aging as well as with gene-regulated processes.⁶ Our study demonstrated that the phenomenon was already present after 24 hr following a single 9-min vessel exposure to calcium chloride and that it progressed significantly to a more organized pattern following the next 30 days. This implies that several unknown factors might be present and play a significant role in arterial medial calcification. Our model has, thus, the potential to be a source of future research for unraveling such factors. It is interesting, nevertheless, to note that calcification could be seen after 24 hr on histopathology (Von Kossa positive) but not on OCT (in vitro). This could represent a rapid absorption of small quantities of calcium by the tunica media through endoluminal exposure given the affinity of elastin and calcium.⁹

Calcified lesions are associated with worsened prognosis overall and have been shown to be independent predictors of stent thrombosis and ischemia driven target lesion revascularization in patients with coronary disease.⁷ Furthermore, the severity of calcification and its luminal topography represent a significant challenge to percutaneous intervention affecting the intervention strategy. Several dedicated devices like eximer laser, rotational and orbital atherectomy, shockwave lithoplasty, cutting, and scoring balloons, have been developed and are currently used to better prepare the calcified lesion for stenting or drug delivery through drug-eluting balloons.²³⁻²⁵ The development and testing of such devices could use such animal model for their perfection before human clinical use.

Additionally, the present model could potentially be used for medical education, especially of fellows and young interventionalists. Some of these dedicated devices have learning curves that require extensive training; and these training programs in real patients are sometimes hazardous, expensive, and cumbersome, disadvantages that could potentially be mitigated by the use of the present animal model.

Our study should be assessed in light of some limitations. First, the proposed model resembles medial calcification and the results presented here cannot be fully extrapolated for the study of intimal calcification seen in atherosclerotic disease. Second, the effect of different dosages and duration of exposure to calcium chloride was not tested, and neither the effect of drugs that could interfere with the calcium–elastin interaction and potentially elucidate hidden mechanisms. Nevertheless, the robustness of our findings resides on the fact that the model is easily reproducible, not expensive to produce, and results in an early extensive circumferential medial calcification that can be useful for different purposes as discussed above.

5 | CONCLUSION

We developed a low-cost, reproducible model of early carotid medial calcification in pigs. Our model has the potential to help the development of research to unravel mechanisms underlying arterial calcification, the use of current or new devices to treat calcified lesions as well as to serve as an option for training interventionalists on the use of such devices.

CONFLICT OF INTEREST

The authors declare no conflict of interest.

ORCID

Carlos M. Campos  <https://orcid.org/0000-0003-1734-6924>

Fabio Sandoli de Brito Jr  <https://orcid.org/0000-0002-6260-9626>

REFERENCES

1. Suzuki Y, Yeung AC, Ikeno F. The pre-clinical animal model in the translational research of interventional cardiology. *JACC Cardiovasc Interv.* 2009;2(5):373-383.
2. Zaragoza C, Gomez-Guerrero C, Martin-Ventura JL, et al. Animal models of cardiovascular diseases. *J Biomed Biotechnol.* 2011;2011:497841.
3. Demer LL, Tintut Y. Vascular calcification: pathobiology of a multifaceted disease. *Circulation.* 2008;117(22):2938-2948.
4. Huisman J, van der Heijden LC, Kok MM, et al. Impact of severe lesion calcification on clinical outcome of patients with stable angina, treated with newer generation permanent polymer-coated drug-eluting stents: a patient-level pooled analysis from TWENTE and DUTCH PEERS (TWENTE II). *Am Heart J.* 2016;175:121-129.
5. Wayhs R, Zelinger A, Raggi P. High coronary artery calcium scores pose an extremely elevated risk for hard events. *J Am Coll Cardiol.* 2002;39(2):225-230.
6. Wu M, Rementer C, Giachelli CM. Vascular calcification: an update on mechanisms and challenges in treatment. *Calcif Tissue Int.* 2013;93(4):365-373.
7. Genereux P, Madhavan MV, Mintz GS, et al. Ischemic outcomes after coronary intervention of calcified vessels in acute coronary syndromes. Pooled analysis from the HORIZONS-AMI (harmonizing outcomes with revascularization and stents in acute myocardial infarction) and ACUITY (acute catheterization and urgent intervention triage strategy) TRIALS. *J Am Coll Cardiol.* 2014;63(18):1845-1854.
8. Zhan Y, Hou J, Xing L, Zhang Y, Yu H, Yu B. Impact of coronary calcifications 12 months after everolimus-eluting stent implantation: an optical coherence tomography study. *European Heart Journal Supplements.* 2015;17(suppl_F):F24-F31.
9. Basalyga DM, Simionescu DT, Xiong W, Baxter BT, Starcher BC, Vyavahare NR. Elastin degradation and calcification in an abdominal aorta injury model: role of matrix metalloproteinases. *Circulation.* 2004;110(22):3480-3487.
10. Belczak S, Silva ES, Aun R, et al. Endovascular treatment of peripheral arterial injury with covered stents: an experimental study in pigs. *Clinics (Sao Paulo).* 2011;66(8):1425-1430.
11. Sincos IR, Aun R, da Silva ES, et al. Impact of stent-graft oversizing on the thoracic aorta: experimental study in a porcine model. *J Endovasc Ther.* 2011;18(4):576-584.
12. Campos CM, Ishibashi Y, Eggermont J, et al. Echogenicity as a surrogate for bioresorbable everolimus-eluting scaffold degradation: analysis at 1-, 3-, 6-, 12-, 18-, 24-, 30-, 36- and 42-month follow-up in a porcine model. *Int J Cardiovasc Imaging.* 2015;31(3):471-482.
13. Strandberg E, Zeltinger J, Schulz DG, Kaluza GL. Late positive remodeling and late lumen gain contribute to vascular restoration by a

- non-drug eluting bioresorbable scaffold: a four-year intravascular ultrasound study in normal porcine coronary arteries. *Circ Cardiovasc Interv.* 2012;5(1):39-46.
14. Raghavan ML, Webster MW, Vorp DA. Ex vivo biomechanical behavior of abdominal aortic aneurysm: assessment using a new mathematical model. *Ann Biomed Eng.* 1996;24(5):573-582.
 15. Raghavan ML, Kratzberg J, de Tolosa EMC, Hanaoka MM, Walker P, da Silva ES. Regional distribution of wall thickness and failure properties of human abdominal aortic aneurysm. *J Biomech.* 2006;39(16):3010-3016.
 16. Raghavan ML, Hanaoka MM, Kratzberg JA, de Lourdes HM, da Silva ES. Biomechanical failure properties and microstructural content of ruptured and unruptured abdominal aortic aneurysms. *J Biomech.* 2011;44(13):2501-2507.
 17. Lederman A, Saliture Neto FT, Ferreira R, et al. Endovascular model of abdominal aortic aneurysm induction in swine. *Vasc Med.* 2014;19(3):167-174.
 18. Nasu K, Tsuchikane E, Katoh O, et al. Effect of fluvastatin on progression of coronary atherosclerotic plaque evaluated by virtual histology intravascular ultrasound. *JACC Cardiovasc Interv.* 2009;2(7):689-696.
 19. Banach M, Serban C, Sahebkar A, et al. Impact of statin therapy on coronary plaque composition: a systematic review and meta-analysis of virtual histology intravascular ultrasound studies. *BMC Med.* 2015;13:229.
 20. Zeng Y, Tateishi H, Cavalcante R, et al. Serial assessment of tissue precursors and progression of coronary calcification analyzed by fusion of IVUS and OCT: 5-year follow-up of scaffolded and non-scaffolded arteries. *JACC Cardiovasc Imaging.* 2017;10:1151-1161.
 21. Proudfoot D, Shanahan CM. Biology of calcification in vascular cells: intima versus media. *Herz.* 2001;26(4):245-251.
 22. Zeng Y, Cavalcante R, Collet C, et al. Coronary calcification as a mechanism of plaque/media shrinkage in vessels treated with bioresorbable vascular scaffold: a multimodality intracoronary imaging study. *Atherosclerosis.* 2017;269:6-13.
 23. Mintz GS. Intravascular imaging of coronary calcification and its clinical implications. *JACC Cardiovasc Imaging.* 2015;8(4):461-471.
 24. Sotomi Y, Cavalcante R, Shlofmitz RA, et al. Quantification by optical coherence tomography imaging of the ablation volume obtained with the orbital atherectomy system in calcified coronary lesions. *EuroIntervention.* 2016;12(9):1126-1134.
 25. Brodmann M, Werner M, Holden A, et al. Primary outcomes and mechanism of action of intravascular lithotripsy in calcified, femoropopliteal lesions: results of disrupt PAD II. *Catheter Cardiovasc Interv.* 2019;93(2):335-342.

How to cite this article: Abrão SR, Campos CM, Cavalcante R, et al. Percutaneous endovascular delivery of calcium chloride to the intact porcine carotid artery: A novel animal model of arterial calcification. *Catheter Cardiovasc Interv.* 2020;96: E484–E492. <https://doi.org/10.1002/ccd.29070>